# Design and Characterization of 500°C Schmitt Trigger in 4H-SiC

Saleh Kargarrazi[1,a], Luigia Lanni[1,b], and Carl-Mikael Zetterling[1,c]

KTH Royal Institute of Technology , 16440 Kista, Sweden

[a]salehk@kth.se, [b]luigia@kth.se, [c]bellman@kth.se

**Keywords:** SiC, BJT, Schmitt Trigger, High temperature IC

**Abstract.**

Two versions of Schmitt trigger, an emitter-coupled and an operational amplifier (opamp)-based, are implemented in 4H-SiC bipolar technology and tested up to 500 °C. The former benefits the simplicity, smaller footprint, and fewer number of devices, whereas the latter provides better promise for high temperature applications, thanks to its more stable temperature characteristics. In addition, the measurements in the range 25 °C - 500 °C, shows that the opamp-based version provides negative and positive slew rates of 4.8 V/$\mu$s and 8.3 V/$\mu$s, $\sim$8 and $\sim$3 times higher than that of the emitter-coupled version, which are 1.7 V/$\mu$s and 1 V/$\mu$s.

## Introduction

The Schmitt trigger circuit, as an essential building block to maintain noise immunity, was originally proposed in 1937 [1]. Since then, its concept has been widely used in pulse shaping circuits. In particular, Schmitt trigger is the basic component of buffers to reject noise from the input signal. It also can be used to build a relaxation oscillator. Electronic circuits for extreme temperatures have been the focus of many studies so far; among them are TTL and ECL logic in Silicon Carbide [2, 3].

As an attempt to move electronics in hostile environments, two versions of Schmitt trigger in 4H-SiC bipolar technology are demonstrated: an emitter-coupled, referred to as *classic version* throughout the paper, and an opamp-based version, both operational from room temperature up to 500 °C.

## SiC Schmitt trigger design

The classic Schmitt trigger consisting of two bipolar junction transistors (BJTs) in an emitter-coupled configuration and five integrated resistors is shown in Fig. 1(a). $Q_1$ acts as a comparator, with a base as the inverting and an emitter as the non-inverting terminal. $Q_2$ is an emitter-follower stage and is driven by the collector of $Q_1$ through the voltage divider resistors, $R_1$ and $R_2$. Coupling $Q_2$ and $Q_1$ emitters forms a positive feedback loop, and therefore provides hysteresis. The positive feedback leads to current steering from $Q_1, R_{c1}$ to $Q_2, R_{c2}$ branch back and forth in a regenerative manner. In order to study the hysteresis behavior of the circuit, assume that the input voltage starts at zero (level high) and declines toward the negative rail,$V_{EE}$. $Q_1$ is on and saturated, conducting current and providing a low voltage at its collector. This enforces $Q_2$ in cut-off. Assuming $V_{EE}$ to be significantly larger than $V_{ce(sat)}$, the emitter voltage, $V_E$, is:

$$V_E = \frac{R_{c1}}{R_{c1} + R_E||(R_1 + R_2)} V_{EE}. \tag{1}$$

The minimum voltage needed to turn $Q_1$ off (and $Q_2$ on), or the low threshold trigger, is:

$$V_{TL} = \frac{R_{c1}}{R_{c1} + R_E||(R_1 + R_2)} V_{EE} + V_{be(on)}. \tag{2}$$

After the transition, $Q_1$ turns off and $Q_2$ conducts in saturation mode. Again, $V_{ce(sat)}$ and $V_{be(sat)}$ can be neglected in comparison with $V_{EE}$, and the emitter voltage is derived as:

$$V_E = \frac{(R_{c1} + R_1)||R_{c2}}{(R_{c1} + R_1)||R_{c2} + R_E||R_2} V_{EE}. \tag{3}$$

The state transition occurs when the input reaches:

$$V_{TH} = \frac{(R_{c1} + R_1)||R_{c2}}{(R_{c1} + R_1)||R_{c2} + R_E||R_2} V_{EE} + V_{be(on)} \tag{4}$$

that is the high threshold trigger level. Using Eq. 2,4, the required hysteresis width and levels can be achieved by tuning the resistor values.

The other version, whose schematics is shown in Fig. 1(b), uses a general purpose opamp in a positive feedback configuration, which acts as a comparator with hysteresis. It consists of 13 BJTs and 13 integrated resistors. The core of the opamp, except for the biasing of the first stage, has a similar topology to that of $MC1530$ by Motorola. In the opamp-based trigger design, the input is connected to the inverting terminal of the opamp, and the output is connected to the non-inverting terminal through the feedback network. Thereby the positive feedback loop is formed. Assuming considerably high gain for the opamp, when the input ($V_-$) declines from positive (high) toward negative (low) rail, as long as $V_- > V_+$, the output remains at negative level. In that case, $V_+ = R_1/(R_1 + R_2) \cdot V_{EE}$. When $V_-$ reaches this value, output switches from low to high ($V_{EE}$ to $V_{CC}$). This determines the low threshold voltage. On the contrary, when input rises from positive toward negative rail, the transition happens at: $R_1/(R_1 + R_2) \cdot V_{CC}$, that is the high threshold voltage.

The circuits are fabricated on a 100 mm SiC wafer. Cross-sectional view of the used epitaxial structure is shown in Fig. 2(a), and optical image the BJT is presented in Fig. 2(b). All integrated resistors are realized in the highly doped collector layer. Further fabrication details are described in [3, 4]. The optical image of the fabricated chip is shown in Fig. 3. While all the circuit components are integrated on-chip, one end of the resistor feedback in the opamp-based Schmitt trigger is left open, and is externally connected by means of a coaxial cable. This gives the option to characterize the circuit with different sizes of integrated feedback resistors.

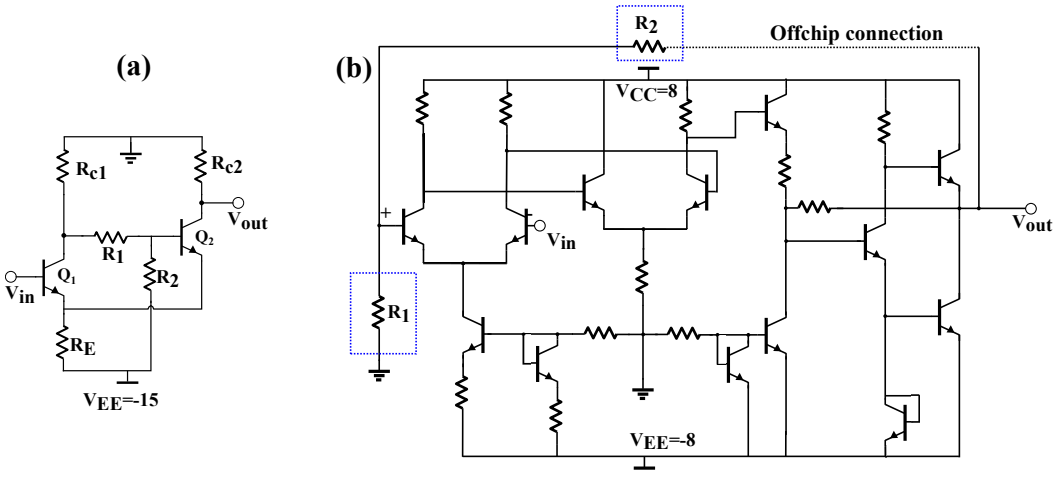


Fig. 1: (a) Schematics of the classic and (b) the opamp-based Schmitt triggers

## Results and discussions

The experimental results are obtained from on-wafer measurements of the chip, placed on a hot stage. The positive supply rail of the classic Schmitt trigger is connected to GND, whereas its negative rail is connected to -15V. Input voltage is swept from -15V to GND and back to -15V, thereby the hysteresis behavior can be derived.

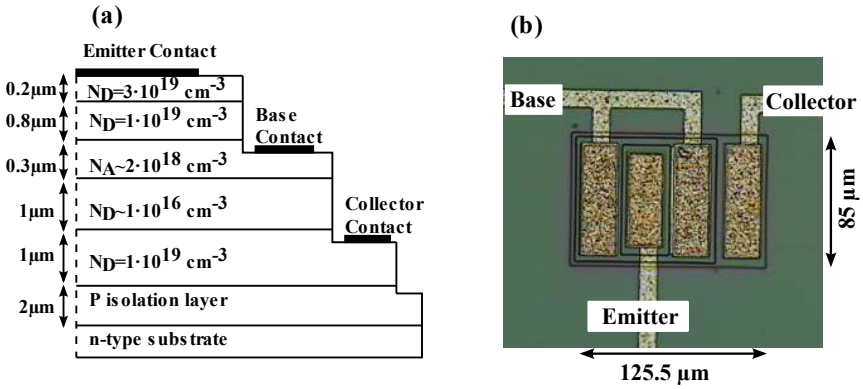


Fig. 2: (a) Cross-sectional view (b) and optical image of the fabricated BJT

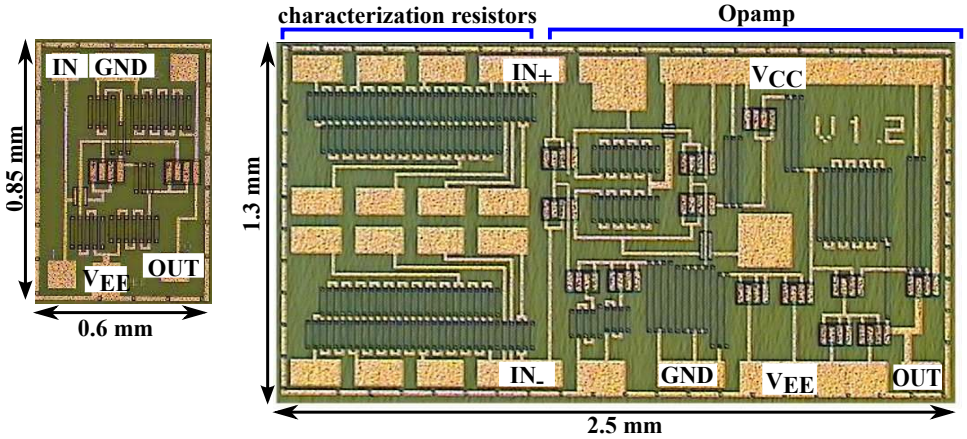


Fig. 3: Optical image of the fabricated chip: the classic Schmitt trigger(left) and the opamp(right)

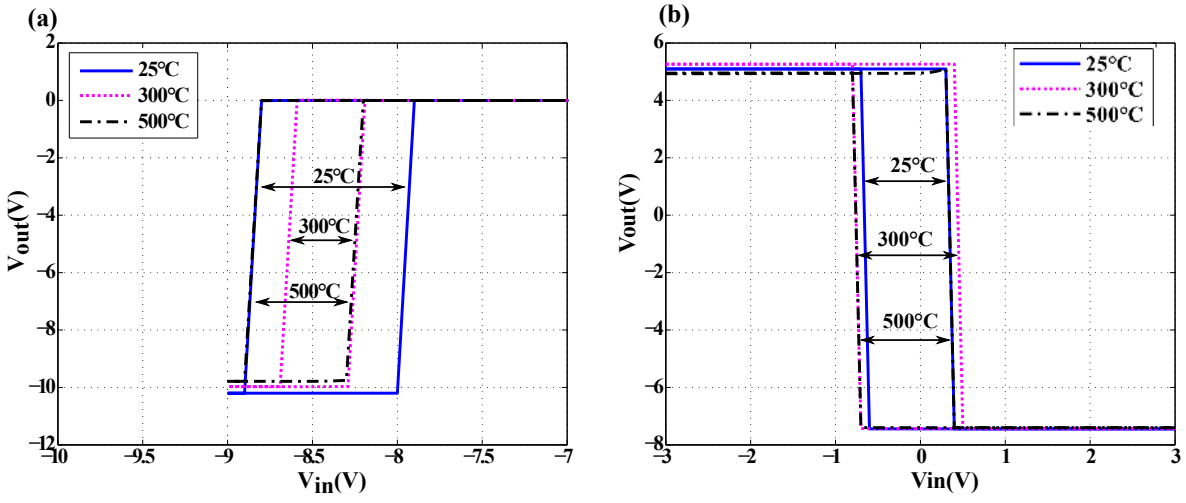


Fig. 4: Measured hysteresis characteristics of (a) the classic (negative supply), and (b) the opamp-based Schmitt triggers

Fig. 4 illustrates the measured transfer curve of the trigger circuits for temperatures ranging from 25° to 500°C for both circuits. A non-monotonous temperature variation of trigger levels in the classic Schmitt trigger is observed that is mainly due to the non-monotonous temperature variation of resistor values and BJTs current gains, as previously shown in this technology[3].

Table 1: Comparison table for the two Schmitt trigger designs

| Design | Temperature performance | Slew Rate (V/$\mu$s) Negative/Positive | Complexity | Area (mm$^2$) | power (mW) (25-500 °C) |
|---|---|---|---|---|---|
| classic (emitter-coupled) | temp. dependent | 1.7/1.0 | 2 BJTs, 5 Resistors | $\sim$0.5 | $\sim$50 |
| opamp-based | temp. independent | 4.8/8.3 | 13 BJTs, 13 Resistors | $\sim$2 | $\sim$160 |

The opamp-based Schmitt trigger is supplied with $\pm$8V power supplies while its input is swept from -3V to 3V and back to -3V. This causes the output voltage to vary from $\sim$5V to $\sim$-7V and back to $\sim$5V . This version of Schmitt trigger, has shown a more robust temperature behaviour comparing with the classic version as depicted in Fig. 4 , thanks to the high overall voltage gain of the opamp, which makes the threshold levels dependent predominantly on the feedback resistor values. Subsequently, since the resistors appear in ratio terms in the equations of the opamp-based version, temperature dependence is mitigated, providing an almost symmetrical hysteresis width of $\sim$1V around the zero voltage in the range 25 °C - 500 °C.

Table. 1 summarizes the the measured characteristics of the two Schmitt triggers. The slew rate (= max$\frac{dV_o}{dt}$) for the two designs in no-load condition is measured by using a square-wave pulse with 1 kHz frequency in the input. The opamp-based Schmitt trigger can provide $\sim$8 and $\sim$3 times higher positive and negative slew rates respectively, compared to the classic version, due to the high current of the output stage and the low output impedance of the emitter follower. The positive and negative values are different, due to the different impedances seen by the output node in rising and falling slopes. Variation of the slew rate by temperature is negligible. Power consumption of both designs, with a 1 kHz square-wave pulse in the input, is measured. The classic version consumes almost 1/3 of power ($\sim$50mW) compared to the opamp-based version($\sim$160mW).

**Summary**

Operation of bipolar Schmitt trigger circuits in 4H-SiC is demonstrated from room temperature up to 500 °C. Two versions, a classic and an opamp-based Schmitt triggers, are designed and characterized. Measurement results show the superiority of the opamp-based version for its higher slew rate and its almost independent temperature operation from 25 °C to 500 °C. The classic version, however, benefits the design simplicity, smaller footprint and lower power consumption.

## References


[1] O. H. Schmitt, ”A thermionic trigger,” *Journal of Scientific Instruments*, vol. 15, no. 1, p. 24, 1938.

[2] S. Singh and J. A. Cooper, ”Bipolar integrated circuits in 4H-SiC,” *Electron Devices, IEEE Transactions on*, vol. 58, no. 4, pp. 1084–1090, 2011.

[3] L. Lanni, B. Malm, M. Ostling, and C.-M. Zetterling, ”500 °C Bipolar Integrated OR/NOR Gate in 4H-SiC,” *Electron Device Letters, IEEE*, vol. 34, no. 9, pp. 1091–1093, 2013.

[4] L. Lanni, B. G. Malm, M. Östling, and C. M. Zetterling, ”SiC etching and sacrificial oxidation effects on the performance of 4H-SiC BJTs,” in *Materials Science Forum*, vol. 778, pp. 1005–1008, Trans Tech Publ, 2014.